Dynamic Behavior of the Well-Mixed Isothermal Crystallizer

M. B. SHERWIN, REUEL SHINNAR, and STANLEY KATZ
City College, City University of New York, New York, New York

Under some conditions, continuous crystallization exhibits cyclic changes of the particle size even with constant input conditions. A linearized stability analysis has been performed to determine under what conditions this behavior can be expected. Numerical solutions of the actual nonlinear system equations were carried out to follow the cyclic behavior and to compute the cycle time and the amplitude of the fluctuations. The effect of seeding on the stability limits and product distribution was also evaluated.

Industrial crystallization operations are still something of an art, and often depend to a considerable degree on the skill of the operator. This paper attempts to aid in the understanding of the dynamic behavior and stability of such systems.

The special feature which distinguishes continuous crystallization processes from other continuous reactors is the simultaneous occurrence of nucleation and growth. Both these steps depend on supersaturation as a driving force, with the rate dependence of nucleation on supersaturation being highly nonlinear. In a well-mixed crystallizer these steps occur simultaneously and homogeneously throughout the vessel.

It has been observed that continuous crystallization processes are under some conditions inherently unstable and of a cyclic nature (*10*). Randolph and Larson (*12*) speculated that the instability and long-term transients in the size distribution observed in an ammonium sulfate crystallizer were due to changes in operation over a three-shift period rather than inherent to the system. Saeman (*10*) found that it was impossible to operate a completely classified ammonium nitrate crystallizer continuously, but was forced to discharge periodically product in a cyclic manner. Changing the operation to a well-mixed crystallizer alleviated, but did not completely remove, the operating problems. Much of this unsteady behavior occurs despite the fact that heat and material inputs and other operating conditions are held constant. Similar observations have been made in some continuous polymerization and fermentation processes which also involve nucleation and growth (*6, 18*).

Theoretical papers on industrial crystallization are very few in number and deal mainly with steady state behavior (*2, 15*). Experimental and theoretical studies on nucleation or growth usually focus on just one of these kinetic steps, thereby avoiding the problem of interaction. This study of the dynamics of the well-stirred crystallizer considers these interactions and tries to analyze what effect variation in operation will have on them. An explanation is proposed for the observed difficulty of attaining continuous stable operation in some cases and means of correcting this behavior become apparent from the text.

Although considerable effort has been spent on the study of the dynamical behavior of both homogeneous and heterogeneous reaction systems (*1, 4, 21*), very few studies deal with the effect of nucleation. Part of this is due to the extreme difficulty in the mathematical treatment of such systems in all but the most simple cases.

Larson (*12*) has made a theoretical linearized stability analysis of a completely mixed crystallizer, and found that under most practical conditions it should be stable. But in an experimental step response study of one typical crystallization, he also found strong tendency toward long-term cyclic transients.

Larson's analysis contains some very strong simplifications, particularly in the neglect of a metastable region of low nucleation rate. It is just this strong nonlinear dependence of nucleation rate on supersaturation that causes the observed cyclic changes in particle size. Our linearized stability analysis allows for such effects, and hence shows both regions of stable and unstable operation.

A linearized stability analysis will only indicate if the system is stable, and will not give any indication as to the magnitude of the fluctuations. Fortunately, for a mixed vessel it is in many cases possible to follow the behavior of a disturbance in the nonlinear region and to compute the amplitude of the fluctuations.

The approach used in this work was presented in a recent paper by Katz and Hulburt (*8*) which allowed a reasonably realistic, theoretical treatment for quite complex situations.

DERIVATION OF THE MODEL

A diagram of the type of operation discussed is shown in Figure 1. A feed material containing solute at concentration c_0 (moles per unit volume) is fed to a crystallizer of working volume V at a volumetric rate ω_0 (volume per unit time). The crystallizer is well mixed and isothermal so that instant cooling of the feed results in a supersaturation driving force for subsequent nucleation and growth. A product slurry representative of the contents of crystallizer body is withdrawn at volumetric rate ω_1.

In order to describe the behavior of the isothermal mixed

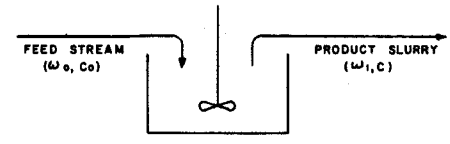

Fig. 1. Mixed crystallizer with mixed-product removal.

M. B. Sherwin is with Chem Systems, Inc., New York, New York.

suspension mixed product removal crystallizer, balances must be written for the particles and the crystallizing material. In addition to these general balances, appropriate kinetic relations must be added for the description to be complete.

In writing these balances the following assumptions were made:

The crystal particles are assumed to be regular solids which maintain their shape upon growth and can therefore be characterized geometrically by a linear dimension r.

For solids which grow in three dimensions, the volume of any crystal is given by Kr^3, where K is the appropriate geometrical shape factor. (This paper will deal with the case of a three-dimensional crystal since it is the most common, although the assumption of plate or needle shaped crystals, which grow in two- and one-dimensions, respectively, could just as easily be substituted.)

The crystal density ρ is taken to be constant.

The particle size distribution is the number density f at size r, such that $f(r, t)\,dr \doteq$ the number of crystals per unit volume of crystallizer having radii in the range r, $r + dr$ at time t.

The fractional volume ε occupied by the solution is a function of time and can be defined in terms of f

$$1 - \varepsilon(t) = \int_0^\infty Kr^3 f(r, t)\,dr \tag{1}$$

Similarly, when a seeded feed is used, $\psi(r, t)\,dr =$ the number of crystals per unit volume of feed having radii in the range r, $r + dr$ at time t and the fractional volume ε occupied by the feed solution is

$$1 - \varepsilon_0(t) = \int_0^\infty Kr^3 \psi(r, t)\,dr \tag{2}$$

The growth rate of an existing crystal dr/dt is assumed to be described by the product of a function of crystal environment $G(c)$ and a function of crystal size $\phi(r)$ such that

$$\frac{dr}{dt} = G(c)\,\phi(r) \tag{3}$$

where c is the solute concentration per volume of solution.

The nucleation rate for new crystals is mainly a function of solute concentration in the crystallizer according to the classical theories of Volmer (*19*) and Mier (*20*). It is assumed that the size distribution of new crystals appears as a Dirac delta function, or that all new crystals are formed at a nominal size r_0.

$B(c)$ = number of crystals born per volume of solution per unit time at r_0. ω_0 and ω are the volumetric feed and withdrawal rates to and from the crystallizer working volume V.

Conservation Equations

Now the appropriate balances over the crystallizer can be written down. (A detailed derivation of the particle balance can be found in reference *8*.)

Particle balance:

$$\frac{\partial[Vf]}{\partial t} + \frac{\partial[G\phi Vf]}{\partial r} = \varepsilon VB\delta(r - r_0) - \omega_1 f + \omega_0 \psi \tag{4}$$

These terms represent, in order, the accumulation of crystals at size r, the net flux of crystals away from size r due to growth, the input of particles at size r_0 due to nucleation, the withdrawal of particles of size r due to product removal, and the input of particles of size r due to solids in the feed.

Solute and crystal balance:

$$\frac{d}{dt}[V\{\varepsilon c + (1 - \varepsilon)\rho\}] = \omega_0[\varepsilon_0 c_0 + (1 - \varepsilon_0)\rho] - \omega_1[\varepsilon c + (1 - \varepsilon)\rho] \tag{5}$$

These terms represent, in order, the accumulation of solute and crystal, the input of solute and crystal by the feed stream, and the removal of solute and crystal due to product withdrawal.

When Equation (4) is multiplied by Kr^3 and integrated over r, the following relation is obtained:

$$\frac{d}{dt}[(1 - \varepsilon)V] = GV\sigma + \varepsilon VBKr_0^3 + \omega_0(1 - \varepsilon_0) - \omega_1(1 - \varepsilon) \tag{6}$$

where

$$\sigma = 3K\int_0^\infty r^2 f\phi\,dr \tag{7}$$

If a balance were written for the solvent and this relation combined with (5) and (6), one could obtain an expression for the variation of the working volume V with time. The resulting expression is

$$\frac{dV}{dt} = (\omega_0 - \omega_1) + (1 - \bar{v}\rho)(\sigma VG + \varepsilon VBKr_0^3) \tag{8}$$

where $\bar{v}$ is the partial molar volume of the solute. Available data indicate that taking $\bar{v} = 1/\rho$ is quite a reasonable assumption, so that if we specify that $\omega_0 = \omega_1 = \omega$, the working volume remains constant.

It is desirable to have a relation expressing the variation of solute concentration c with time, since both G and B are expressed in terms of this variable. Equations (5) and (6) can be used along with the assumption of constant volume to yield the desired expression:

$$\varepsilon\frac{dc}{dt} = \frac{\omega}{V}(c_0 - c)\,\varepsilon_0 - (\rho - c)(\sigma G + \varepsilon BKr_0^3) \tag{9}$$

The working set of equations is now

$$\frac{\partial f}{\partial t} + \frac{\partial}{\partial r}[G\phi f] = \varepsilon B\delta(r - r_0) + \frac{\psi}{\theta} - \frac{f}{\theta} \tag{10}$$

$$\varepsilon\frac{dc}{dt} = \frac{(c_0 - c)\varepsilon_0}{\theta} - (\rho - c)(\sigma G + \varepsilon BKr_0^3) \tag{11}$$

where

$$\theta = \frac{V}{\omega}$$

$$\sigma = 3K\int_0^\infty r^2 f\phi\,dr$$

Moment Equations

The above set of equations is difficult to solve, even numerically, since it contains a partial differential equation for $f(r, t)$. If it is not necessary to determine how the distribution f varies with time, but a knowledge of the variation of its moments with time is satisfactory, the set can be transformed to a group of ordinary differential equations. The n^{th} moment of f will be called μ_n while the expressions in pointed brackets are averages over f in the same sense; in general

$$\langle\eta\rangle = \int_0^\infty \eta f\,dr \tag{12}$$

$$\mu_n(t) = \int_0^\infty r^n f(r, t)\,dr \tag{13}$$

The physical significance of the moments of f is shown below:

$$\mu_0 = \int_0^\infty f\,dr = \text{total number of crystals per unit volume of crystallizer}$$

$$\mu_1 = \int_0^\infty r f\,dr = \text{total radius of crystals per unit volume of crystallizer}$$

$$3K\mu_2 = 3K\int_0^\infty r^2 f\,dr = \text{total surface of crystals per unit volume of crystallizer}$$

$$K\mu_3 = K\int_0^\infty r^3 f\,dr = (1-\varepsilon) = \text{volume fraction of solids}$$

In the same manner, the moments of the seed crystal distribution can be written as

$$\eta_n(t) = \int_0^\infty r^n \psi(r,t)\,dr \tag{14}$$

and these moments retain the same physical significance as the corresponding moments related to f per unit volume of feed.

The weight distribution of the crystals $W(r)$ can be written as

$$W(r) = \rho K r^3 f(r) \tag{15}$$

so that the mean particle size with respect to the weight distribution is

$$\text{Mean particle size} = r_{wm} = \frac{\int_0^\infty rW(r)\,dr}{\int_0^\infty W(r)\,dr} = \frac{\rho K\int_0^\infty r^4 f(r)\,dr}{\rho K\int_0^\infty r^3 f(r)\,dr} = \frac{\mu_4}{\mu_3} \tag{16}$$

The variance of the weight distribution is

$$\text{Variance} = \frac{\int_0^\infty (r-r_{wm})^2 W(r)\,dr}{\int_0^\infty W(r)\,dr} = \frac{\int_0^\infty r^2W(r)\,dr - 2r_{wm}\int_0^\infty W(r)\,dr + r_{wm}^2\int_0^\infty W(r)\,dr}{\int_0^\infty W(r)\,dr} \tag{17}$$

which, in terms of the number distribution is

$$\text{Variance} = \frac{\mu_5}{\mu_3} - \left(\frac{\mu_4}{\mu_3}\right) \tag{18}$$

The coefficient of variation γ of the weight distribution is a measure of its uniformity.

$$\gamma^2 = \frac{\text{variance}}{(\text{mean size})^2} = \frac{\dfrac{\mu_5}{\mu_3} - \left(\dfrac{\mu_4}{\mu_3}\right)^2}{\left(\dfrac{\mu_4}{\mu_3}\right)^2} \tag{19}$$

Clearly all these moments in Equations (16), (17), and (19) can be determined by a microscopic analysis of a sieve analysis of the crystallizer product. It is also clear that a knowledge of these moments is enough to characterize the performance of a crystallizer.

By multiplying Equation (10) through by r^n and integrating, one can generate the moment equations:

$$\frac{d\mu_n}{dt} = nG(c)\left\langle r^{n-1}\phi(r)\right\rangle + \varepsilon B(c) r_0^n + \frac{\eta_n}{\theta} - \frac{\mu_n}{\theta} \qquad n = 0, 1, 2, 3 \ldots. \tag{20}$$

where

$$\left\langle r^{n-1}\phi(r)\right\rangle = \int_0^\infty r^{n-1}\phi(r) f\,dr$$

Now the series of Equations (20) plus Equation (11) is the set of equations describing the system. These, however, do not necessarily give a self-contained set of equations because of the dependence of particle growth on r, as manifested in the terms $\left\langle r^{n-1}\phi\right\rangle$. If dr/dt is independent of r, then $\phi = 1$ and $\left\langle r^{n-1}\phi\right\rangle$ is simply μ_{n-1} and the equations close satisfactorily at $n = 3$. This is so even if dr/dt depends linearly on r, but more awkward terms of dependence (r^2, r^3, etc.) can only be handled by making successive approximations to $f(r, t)$ in the term of Laguerre series as discussed in reference *8*.

Fortunately a number of investigators (*9*, *14*, *17*) have found that in many cases the growth rate does not depend on r to any significant amount, so that in the following sections it is assumed that $\phi = 1$.

Later in the paper growth models of the form

$$\frac{dr}{dt} = G(c)[1 + ar] \tag{21}$$

which include a size-dependent term will be studied to illustrate the effect of this dependence.

Remembering that $1 - \varepsilon = \int_0^\infty Kr^3 f\,dr$, we get the following closed set of equations:

$$\begin{aligned}
\frac{d\mu_0}{dt} &= (1 - K\mu_3)B(c) - \frac{\mu_0}{\theta} + \frac{\eta_0}{\theta}\\
\frac{d\mu_1}{dt} &= G(c)\mu_0 + (1 - K\mu_3)B(c) r_0 - \frac{\mu_1}{\theta} + \frac{\eta_1}{\theta}\\
\frac{d\mu_2}{dt} &= 2G(c)\mu_1 + (1 - K\mu_3)B(c) r_0^2 - \frac{\mu_2}{\theta} + \frac{\eta_2}{\theta}\\
\frac{d\mu_3}{dt} &= 3G(c)\mu_2 + (1 - K\mu_3)B(c) r_0^3 - \frac{\mu_3}{\theta} + \frac{\eta_3}{\theta}\\
(1 - K\mu_3)\frac{dc}{dt} &= \frac{(c_0 - c)}{\theta}\varepsilon_0 - (\rho - c)(3G(c)K\mu_2 + (1 - K\mu_3)B(c)Kr_0^3)
\end{aligned} \tag{22}$$

In order to solve this set of equations to trace the history of $c(t)$ and the moments of $f(r, t)$, the system (22) must be supplemented by the initial conditions and the feed rate and composition as a function of time. Also the dependence of $B(c)$ and $G(c)$ on concentration $c(t)$ must be specified.

Steady State Equations

In order to get the steady state moments, the particle distribution $\bar{f}(r)$ must first be obtained. This can then be used to generate the moment relations.

The steady state particle balance can be written down from (10), remembering that we are now assuming $\phi = 1.0$:

$$G(c)\frac{df}{dr} = \varepsilon\beta(c)\delta(r - r_0) - \frac{f(r)}{\theta} + \frac{\psi(r)}{\theta} \tag{23}$$

where the superscript bars indicate steady state values.

This can be solved, giving

$$\bar{f} = \frac{\varepsilon B}{G} e^{-\frac{1}{\theta G}(r - r_0)} + \frac{1}{\theta G}\int_0^r \psi(x)\, e^{-\frac{1}{\theta G}(r-x)}\,dx \tag{24}$$

The moments can now be obtained by straightforward calculation from (24):

$$\bar{\mu}_0 = \frac{\varepsilon B}{G}(\theta G) + \eta_0$$

$$\bar{\mu}_1 = \frac{\varepsilon B}{G}(\theta G)^2\left[\left(\frac{r_0}{\theta G}\right) + 1\right] + \theta G\eta_0 + \eta_1$$

$$\bar{\mu}_2 = \frac{\varepsilon B}{G}(\theta G)^3\left[\left(\frac{r_0}{\theta G}\right)^2 + 2\left(\frac{r_0}{\theta G}\right) + 2\right] + 2(\theta G)^2\eta_0 + 2\theta G\eta_1 + \eta_2 \tag{25}$$

$$\bar{\mu}_3 = \frac{\varepsilon B}{G}(\theta G)^4\left[\left(\frac{r_0}{\theta G}\right)^3 + 3\left(\frac{r_0}{\theta G}\right)^2 + 6\left(\frac{r_0}{\theta G}\right) + 6\right] + 6(\theta G)^3\eta_0 + 6(\theta G)^2\eta_1 + 3(\theta G)\eta_2 + \eta_3 \quad \text{etc.}$$

An additional relation which will be of use later is derived from the last two relations in set (22).

$$\bar{\varepsilon} = 1 - K\bar{\mu}_3 = \left(\frac{\rho - \bar{c}_0}{\rho - \bar{c}}\right)\bar{\varepsilon}_0 \tag{26}$$

LINEARIZATION OF THE MODEL

In order to determine under what conditions instability in the system will occur, the set of equations describing the system (22) must be linearized about the steady state. Then the conditions under which a small displacement from the steady state will grow may be determined via the conventional use of the Routh-Horwitz criterion. Primed quantities indicate the departure from the steady state values (superscript bar). The feed rate and concentration can vary in time in the form

$$\omega(t) = \bar{\omega} + \omega'(t)$$
$$c_0(t) = \bar{c}_0 + c_0'(t) \tag{27}$$

The initial conditions are

$$c(0) = \bar{c}$$
$$\mu_n(0) = \bar{\mu}_n \quad n = 0, 1, 2, \ldots \tag{28}$$

The performance variables are represented by

$$\mu_n(t) = \bar{\mu}_n + \mu_n' \quad n = 0, 1, 2, \ldots$$
$$c(t) = \bar{c} + c'(t) \tag{29}$$

The kinetic terms for small displacements can be written as

$$B(c) = \bar{B} + \frac{dB}{dc}(c)\cdot c'$$
$$G(c) = \bar{G} + \frac{dG}{dc}(c)\cdot c' \tag{30}$$

In addition, the following dimensionless variables are defined:

$$g = \frac{\bar{\varepsilon}_0(1 - \bar{\varepsilon})}{\bar{\varepsilon}(\varepsilon_0 - \bar{\varepsilon})}\frac{\bar{c}_0 - \bar{c}}{\bar{G}}\frac{dG}{dc}(\bar{c}) \tag{31}$$

$$b = \frac{\bar{\varepsilon}_0(1 - \bar{\varepsilon})}{\bar{\varepsilon}(\varepsilon_0 - \bar{\varepsilon})}\frac{\bar{c}_0 - \bar{c}}{\bar{B}}\frac{dB}{dc}(\bar{c}) \tag{32}$$

where

$$\varepsilon = 1 - K\mu_3$$
$$\varepsilon_0 = 1 - K\eta_3$$
$$Z_n' = \frac{\mu_n'}{\bar{\mu}_n}$$
$$Y' = \frac{\bar{\varepsilon}(\bar{\varepsilon}_0 - \bar{\varepsilon})}{\bar{\varepsilon}_0(1 - \bar{\varepsilon})}\frac{c'}{\bar{c}_0 - \bar{c}} \tag{33}$$

$$\tau = t\bar{\omega}/V = t/\theta$$
$$p(\tau) = \frac{\omega'(\tau)}{\bar{\omega}}$$
$$q(\tau) = \frac{(\bar{\varepsilon}_0 - \bar{\varepsilon})}{(1 - \bar{\varepsilon})}\frac{c_0'(\tau)}{\bar{c}_0 - \bar{c}}$$

Now substitution of Equations (27) to (33) into (22) and utilization of the steady state relations result in the following dimensionless and linearized set:

$$\frac{dZ_n'}{d\tau} - \left[\left(\overline{n\frac{\mu_{n-1}}{\mu_n}\theta G}\right)g + \left(\overline{1 - \frac{\eta_n}{\mu_n}}\right)b - \left(\overline{n\frac{\mu_{n-1}}{\mu_n}\theta G}\right)b\right]Y' - \left[\overline{n\frac{\mu_{n-1}}{\mu_n}\theta G}\right]Z_{n-1} + \left[\overline{Kr_0nB\theta\frac{\mu_3}{\mu_n}}\right]Z_3 + Z_n = -p(\tau)\left[\overline{1 - \frac{\eta_n}{\mu_n}}\right] \quad n = 0, 1, 2, \ldots.$$

with $Z_n'(0) = 0$

$$\frac{dY'}{d\tau} + \left[\left(\overline{3\frac{\mu_2}{\mu_3}\theta G}\right)g + \left(\overline{1 - \frac{\eta_3}{\mu_3}}\right)b - \left(\overline{3\frac{\mu_2}{\mu_3}\theta G}\right)b\right]Y' + Y' + \left[\overline{3\frac{\mu_2}{\mu_3}\theta G}\right]Z_2' - \overline{[Kr_0{}^3B\theta]}Z_3' = q(\tau) + \left[\overline{1 - \frac{\eta_3}{\mu_3}}\right]p(\tau) \tag{34}$$

with $Y'(0) = 0$

There are three sets of dimensionless groups containing steady state variables which arise in (34):

$$L_n = n\frac{\bar{\mu}_{n-1}}{\bar{\mu}_n}\bar{\theta}\bar{G} \quad n = 0, 1, 2, \ldots \tag{35}$$

$$R_n = Kr_0{}^3\bar{B}\bar{\theta}\frac{\bar{\mu}_3}{\mu_n} \tag{36}$$

$$S_n = \frac{\bar{\eta}_n}{\bar{\mu}_n} \tag{37}$$

besides the dimensionless kinetic parameters b and g which have been defined in Equations (31) and (32).

These sets of dimensionless groups L_n, R_n, and S_n depend on a finite number of steady state parameters contained in Equation (25). The identification and dependence of the model on these parameters will be discussed in succeeding sections.

KINETIC MODELS

Some well-known growth and nucleation models are now briefly introduced and substituted into Equations (31) and (32) in order to relate these important dimensionless kinetic parameters to the variables of the system.

It should be mentioned here that the later sections will show that the ratio of these two groups, b/g, is of primary importance in determining the stability and dynamic behavior of the model.

Growth Model

Many investigators have found the relation between G and c to be satisfied by

$$G(c) = K_1(c - c_s) \tag{38}$$

where K_1 is a constant for isothermal operation and c_s is the solubility concentration of the solute. Substitution of this model into Equation (31) yields

$$g = \frac{\bar{\varepsilon}_0(1-\bar{\varepsilon})}{\bar{\varepsilon}(\bar{\varepsilon}_0-\bar{\varepsilon})}\frac{(\bar{c}_0-\bar{c})}{(\bar{c}-c_s)} \tag{39}$$

Generally, the supersaturation $(c - c_s)$ of crystallizing systems is quite small when compared with the difference between feed and outlet concentrations, so that normally the value of g should be of the order of magnitude 10^2 to 10^3.

Nucleation Models

Volmer's model (*15*) is based on thermodynamic considerations and gives rise to an Arrhenius type of function:

$$B = K_2 e^{\frac{K_3}{(\ln c/c_s)^2}} \tag{40}$$

Substitution of this model into Equation (32) yields

$$b = \frac{\bar{\varepsilon}_0(1-\bar{\varepsilon})}{\bar{\varepsilon}(\bar{\varepsilon}_0-\bar{\varepsilon})}\frac{(\bar{c}_0-\bar{c})2K_3}{\bar{c}[\ln \bar{c}/c_s]^2} \approx \frac{\bar{\varepsilon}_0(1-\bar{\varepsilon})}{\bar{\varepsilon}(\bar{\varepsilon}_0-\bar{\varepsilon})} \times \frac{\bar{c}_0-\bar{c}}{\bar{\varepsilon}}\frac{2K_3}{\bar{c}(\bar{c}/c_s-1)^3} \tag{41}$$

the latter approximation being made since $(c/c_s - 1)$ is very small for crystallization systems.

Then using the kinetic models given by Equations (38) and (40), we can approximate the term b/g by

$$\frac{b}{g} = \frac{2K_3(\bar{c}-c_s)}{(\bar{c}/c_s-1)^3\bar{c}} = \frac{2K_3 c_s}{(\bar{c}/c_s-1)^2\bar{c}} \approx \frac{2K_3}{(\bar{c}/c_s-1)^2} \tag{42}$$

The term b/g represents the sensitivity ratio of the nucleation to growth functions at the steady state conditions and it can be seen that, as the solute concentration approaches its solubility limit, this term rapidly increases in value.

Another nucleation model which is a simplified representation of Equation (40) is Mier's metastable model (*16*) which can be written as

$$\begin{aligned} B &= K_4(c-c_m)^m \qquad c > c_m \\ B &= 0 \qquad\qquad\quad c \le c_m \end{aligned} \tag{43}$$

where k_4 is a constant, c_m is the metastable concentration, above which nucleation occurs, and m is some power. Combining this with Equation (38) we get

$$\frac{b}{g} = m\frac{\bar{c}-c_s}{\bar{c}-c_m} \qquad c > c_m \tag{44}$$

Here it is evident that as the solute concentration approaches the metastable limit c_m from above, the sensitivity ratio b/g will increase in value.

It should be pointed out that nucleation in a mixed crystallizer is a highly complex phenomenon involving both homogenous and heterogenous nucleation, the latter being the preferential formation of nuclei near a surface of the same crystals. As Equation (40) was derived for homogenous nucleation one could therefore question its application to nucleation in a crystal magma.

In the strict theoretical sense, Vollmer's equation with its theoretically derived constants is not applicable. In the same way no data obtained from nucleation of a clear solution can be applied to the design of a continuous crystallizer.

In a heterogenous nucleation process, the nucleation rate should depend on both concentration and total crystal surface. In the presence of a large amount of crystals, the dependence on surface is a small effect as compared with the very strong and nonlinear dependence on supersaturation. Rumford and Bain (*14*) have investigated the nucleation of sodium chloride in a bed of large crystals and found that the dependence of the nucleation rate on supersaturation is very similar to that of homogenous nucleation. There is a pronounced measurable metastable supersaturation, (1.5 g. of salt/liter), below which nucleation is negligible and above which its rate increases rapidly and almost linearly with supersaturation. Close to the metastable region Equations (40) and (43) express therefore equally well the basic behavior of a nucleation process in a crystal magma. The advantage of using Equation (40) in a dynamic study is that it is smooth over the whole concentration range.

Larson (*12*) has suggested that the nucleation rate can be approximated by substituting c_s instead of c_m into Equation (43):

$$B = K(c-c_s)^m$$

This leads to a significant simplification of the mathematics, as now B can be expressed as a simple function of G. However, this approximation is only valid when $c_m - c_s$ is very small as compared with $c - c_s$. This might apply to precipitation of very insoluble compounds but is hardly a valid assumption for crystallizers which in most cases operate very closely to the metastable range (*14*).

STABILITY ANALYSIS

Clear Feed

The simplification of a clear feed, such as that $\varepsilon_0 = 1.0$ is imposed here. Many crystallizers operate in this manner since it alleviates the problem of preparing and metering seed nuclei into the system. This assumption means the following:

$$\begin{aligned} \psi &= 0 \\ \eta_n &= 0 \qquad n = 0,1,2,\ldots \\ \varepsilon_0 &= 1.0 \end{aligned}$$

which considerably simplified the relations previously derived.

The dimensionless groups arising in the set of linearized Equations (34) reduced to two, L_n and R_n, as defined in Equations (35) and (36) since the S_n are zero for the clear feed case. Before substituting the steady state relations (25) into (35) and (36) to determine L_n and R_n, we define a new group α:

$$\alpha = \left(\frac{\bar{\omega}}{V\bar{G}}r_0\right) = \frac{r_0}{\bar{\theta}\bar{G}} \tag{45}$$

This group is the ratio of the nuclei radius divided by the steady state growth, per draw-down time $v/\bar{\omega}$. Now substituting (25) and (45) and (36), we get

$$\begin{aligned} L_0 &= 0 \\ L_1 &= 1/(\alpha+1) \\ L_2 &= 2(\alpha+1)/(\alpha^2+2\alpha+2) \\ L_3 &= 3(\alpha^2+2\alpha+2)/(\alpha^3+3\alpha^2+6\alpha+6) \end{aligned} \tag{46}$$

$$\begin{aligned} R_0 &= (1-\bar{\varepsilon})/\bar{\varepsilon} \\ R_1 &= (1-\bar{\varepsilon})\alpha/\bar{\varepsilon}(\alpha+1) \\ R_2 &= (1-\bar{\varepsilon})\alpha^2/\bar{\varepsilon}(\alpha^2+2\alpha+2) \\ R_3 &= (1-\bar{\varepsilon})\alpha^3/\bar{\varepsilon}(\alpha^3+3\alpha^2+6\alpha+6) \end{aligned} \tag{47}$$

The groups L_n are functions of α only, while R_n are functions of both α and $\bar{\varepsilon}$. Values of L_n and R_n for the

fourth and fifth moments can also be found without difficulty, when needed.

The closed set of linearized equations can now be written as

$$\frac{dZ_0'}{d\tau} + Z_0' + R_0 Z_3' - bY' = -p(\tau)$$

$$\frac{dZ_1'}{d\tau} - L_1 Z_0' + Z_1' + R_1 Z_3' - [L_1 g + (1 - L_1)\, b]\, Y' = -p(\tau)$$

$$\frac{dZ_2'}{d\tau} - L_2 Z_1' + Z_2' + R_2 Z_3' - [L_2 g + (1 - L_2)\, b]\, Y' = -p(\tau) \qquad (48)$$

$$\frac{dZ_3'}{d\tau} - L_3 Z_2' + [1 + R_3] Z_3' - [L_3 g + (1 - L_3)\, b]\, Y' = -p(\tau)$$

$$\frac{dY'}{d\tau} + L_3 Z_2' - R_3 Z_3' + [L_3 g + (1 - L_3)\, b + 1]\, Y' = p(\tau) + q(\tau)$$

The eigenvalues of this set of equations can be found directly or the set of linear differential equations can be reduced to a set of algebraic equations by taking the Laplace transforms. In the latter case, the location of the poles of the transfer function would determine the stability of the system.

α, $\bar{\varepsilon}$, b, and g are the parameters of the system which determine the location of the poles of the transfer function. The results of applying the Routh-Horwitz criterion to this set of equations are presented in Figures 2 and 3. It is very surprising (Figure 2) that $\bar{\varepsilon}$ has such a negligible effect on the limits of stable operation.

It was found that for small values of α (which is most pertinent to crystallization), the ratio of b/g reached a limiting value with increasing values of g. For this reason

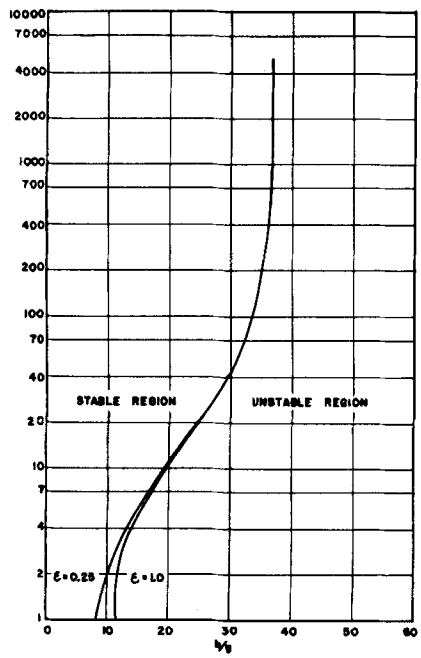

Fig. 2. Stability limits as a function of liquid volume fraction ϵ ($\alpha = 0.1$).

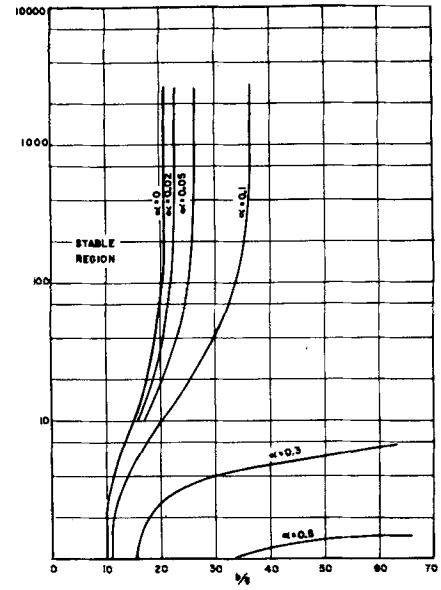

Fig. 3. Stability limits as a function of nuclei size parameter α ($\epsilon = 0.8$).

Figures 2 and 3 indicate g and b/g as the system parameters, rather than g and b. For high values of g, (which is expected), the stability depends on the single parameter b/g (critical) which is a unique function of α or the ratio of nuclei size to the average linear size increase of a crystal per draw-down time (Figure 3).

For most crystallization systems α will have values close to zero and in the past investigators (*2, 12, 15*) have taken α equal to zero. In some cases there is however a justification to consider values of α different from zero. Consider for example the case in which the growth rate is controlled by mass transfer to the surface. For particles which are large as compared with the microscale of turbulence (*16*) the mass transfer rate is independent of diameter. For small particles it is inversely proportional to particle size. To investigate the effect of the highly linearized growth rate of small particles on the dynamic behavior of the system, one can approximate the nonlinear dependence of G on r by a step function at which G is very large for $r < r_0$ and independent of r for $r > r_0$. This is equivalent to saying that the nuclei are really created at size r_0 which could be as large as 1 to 10 micra.

Seeded Feed

For the special case when the seed size is identical to the generated nuclei size (both distributions appearing as delta functions), the equations of the preceding section can be used to predict the effect of seed addition on the system's stability. The nucleation term $B(c)$ is expanded to include all nuclei entering the system as shown below.

$$B(c)_{\text{total}} = B(c)_{\text{nucleated}} + \frac{\psi\, \omega/V}{\varepsilon} \qquad (49)$$

where ψ is defined to be the number of seeds per unit volume of feed so that $(\psi\, \omega/V/\varepsilon)$ is the seed addition rate per unit volume of crystallizer solution.

If we represent the steady state number of seeds as equal to ζ time the generated nuclei (bar indicates steady state values)

$$\frac{\bar{\psi}\, \bar{\omega}/V}{\bar{\varepsilon}} = \zeta \bar{B}(c)_{\text{nucleated}} \quad \zeta > 0 \qquad (50)$$

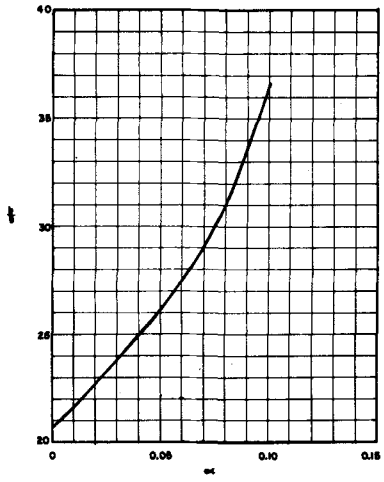

Fig. 4. Limiting values of b/g vs. α ($0 \leq \alpha \leq 0.1$).

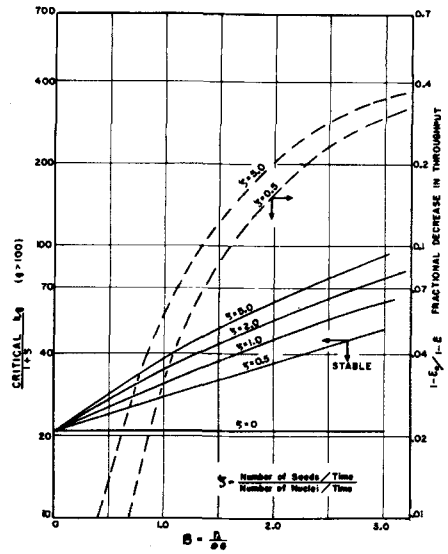

Fig. 5. Effect of seeding on stability and throughput.

so that

$$\overline{B}(c)_{\text{total}} = (\zeta + 1)\,\overline{B}(c)_{\text{nucleated}} \tag{51}$$

the sensitivity coefficient b/g for the seeded case will be less than the sensitivity coefficient for the unseeded case at identical supersaturations.

$$\left(\frac{b}{g}\right)_{\text{seeded}} = \frac{1}{1+\zeta}\left(\frac{b}{g}\right)_{\text{unseeded}} \tag{52}$$

Therefore at identical superation levels seed addition will increase the stability limits of a crystallizer while at the same time it reduces the weight mean particle size.

To determine the stability boundaries of the seeded system when the seed size is different from the nuclei size, it is necessary to return to the set of linearized Equations (34) and their associated dimensionless groups L_n, R_n, and S_n as given in Equations (35) to (37).

In order to evaluate these groups one can simplify matters by assuming that the seed distribution is a delta function at seed size r_s, such that

$$\eta_n = \int \psi(r)\,\delta(r - r_s)\,r^n\,dr = r_s^{\,n}\psi \tag{53}$$

Then two new steady state dimensionless groups are defined:

$$\beta = \overline{\omega} r_s / V\overline{G} = \frac{r_s}{\overline{\theta}\,\overline{G}} \tag{54}$$

$$\zeta = \overline{\psi}(\overline{\omega}/V)/\overline{\varepsilon}\,B = \overline{\psi}/\overline{\theta}\,\overline{\varepsilon}\,\overline{B} \tag{55}$$

The first of these β is similar to α defined in Equation (45) and is the ratio of the seed size to the steady state size increase per draw-down time. The second group ζ is the ratio of the seed addition rate per unit volume of crystallizer to the nuclei generation rate per unit volume of crystallizer. Substituting (45), (54), and (55) into the steady state moment relations (25), we simplify their representation as shown below:

$$\begin{aligned}
\overline{\mu}_0 &= \overline{\varepsilon}\,\overline{\beta}\,\overline{\theta}(1+\zeta) \\
\overline{\mu}_1 &= \overline{\varepsilon}\,\overline{\beta}\,\overline{\theta}\,(\overline{\theta}\,\overline{G})\,[(\alpha+1) + \zeta(\beta+1)] \\
\overline{\mu}_2 &= \overline{\varepsilon}\,\overline{\beta}\,\overline{\theta}\,(\overline{\theta}\,\overline{G})^2\,[(\alpha^2+2\alpha+2) + \zeta(\beta^2+2\beta+2)] \quad \text{etc.}
\end{aligned} \tag{56}$$

so that

$$L_n = n\,\overline{\theta}\,\overline{G}\,\frac{\overline{\mu}_{n-1}}{\overline{\mu}_n} = \text{funct. } (\alpha, \beta, \zeta)$$

$$R_n = K\,\frac{\overline{\mu}_3}{\overline{\mu}_n}\,r_0^{\,n}\,\overline{\theta}\,\overline{B} = \frac{1-\overline{\varepsilon}}{\overline{\mu}_n}\,r_0^{\,n}\,\overline{\theta}\,\overline{B} = \text{funct. } (\alpha, \beta, \zeta, \varepsilon) \tag{57}$$

$$S_n = \frac{\overline{\eta}_n}{\overline{\mu}_n} = \frac{r_s^{\,n}\overline{\psi}}{\overline{\mu}_n} = \text{funct. } (\alpha, \beta, \zeta)$$

The behavior of the linearized equations describing the seeded case is determined by the parameters α, β, $\overline{\varepsilon}$, ζ, g, and b; the two new groups β and ζ are added to characterize the seed size and quantity.

The stability boundaries for the seeded feed was investigated for a number of cases and the results are presented in Figure 4. These curves are for a nuclei size of zero ($\alpha = 0$) and a value of $g = 500$. The stability boundaries, as in the unseeded case, are relatively insensitive to variations in $\overline{\varepsilon}$ and g (when g is greater than 100). The stability limits increase with increasing seed number and seed size, both of which contribute to increasing surface area. However, larger seed sizes ($\beta > 1.0$) are not realistic since for a fixed feed rate or draw-down time the net throughput of product is diminished. Figure 5 also shows this relation by plotting the ratio of the crystal fraction of the feed over that of the product stream, against seed size at two levels of seed addition. The ordinate represents the loss of production capacity due to seeding.

Size-Dependent Growth Model

In the previous calculations it was assumed that the linear growth rate is independent of size. This assumption is correct if the rate determining step is the kinetic deposition rate of the surface. It has also been shown experimentally that for large crystals ($d \gg 100\mu$) the overall mass transfer coefficient at high agitation rates is independent of size. For very small crystals this assumption probably does not hold. As mentioned previously if the growth rate is size dependent the analytical treatment becomes much more complicated, as the first four moments equations plus the solute balance equation are no longer a

closed set of equations. However it is possible to estimate the nature of the effect of size dependent growth rates on stability by linearizing the growth function $\frac{dr}{dt}(r, c)$. If one can approximate $\frac{dr}{dt}(r, c)$ by

$$\frac{dr}{dt} = G(c)\,\phi(r) = G(c)\,(1 + ar) \tag{58}$$

then the set of Equations (11) and (20) will still give a self contained set.

When performing the calculations for this case it was assumed that the term $aG\theta$ was small, that is, of the order of ± 0.1 or less. The group $aG\theta$ is the relative size increase per draw-down time due to the size-dependent term ar, and the assumption that its value remains small is synonymous with the assumption that we are investigating a first-order correction of the size-independent ($\phi = 1$) growth model.

Figure 6 shows the effect of the size-dependent term on the stability contours for nonseeded operation with the nuclei size (α) equal to zero. It is seen that a model which predicts increasing growth rate with increasing size raises the system's stability limits. Based on the previous results this is to be expected, since it should lead to a shorter time lag between the appearance of increased nuclei and increased surface area in the system.

Operation with a Fines Trap

In order to increase crystal product size many crystallization systems utilize a nuclei trap. This usually consists of withdrawing solution from some part of the vessel in such a manner that only crystals below a certain size will be elutriated with the solution. This stream is heated to redissolve the solids and then returned to the crystallizer body. Most often this operation is carried on continuously rather than on the basis of some feedback signal. The question we wanted to answer at present is whether this continuous nuclei removal operation would increase or decrease the system's stability.

In order to dissolve the nuclei they must be trapped very

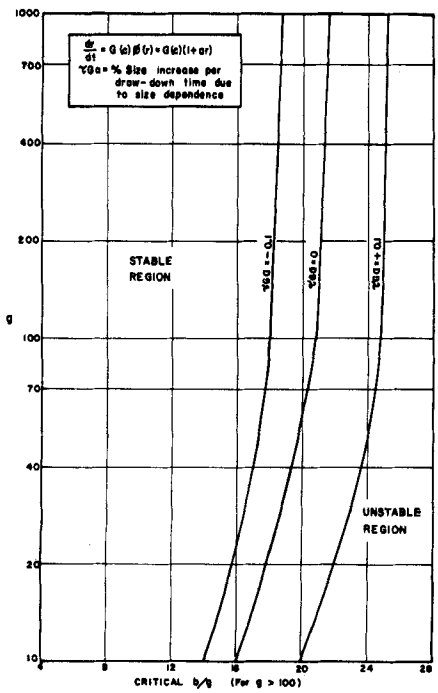

Fig. 6. Effect of linear $\phi(r)$ on stability.

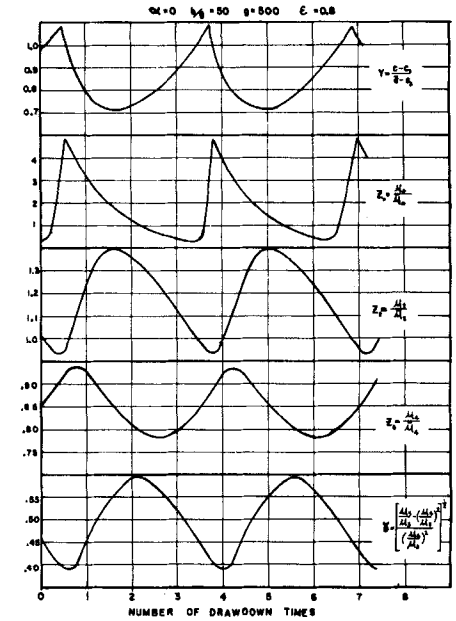

Fig. 7. Typical limit cycle behavior. $\alpha = 0$, $b/g = 50$, $g = 500$, $\epsilon = 0.8$.

early, before they have a chance to grow, say within $\frac{1}{8}$ to $\frac{1}{4}$ of a draw-down time θ. Figure 7 indicates that over this time period, even for cycling behavior, the variation in supersaturation or growth rate $G(c)$ is relatively small. We therefore assume a quasi steady state condition such that the fraction of new nuclei being generated at a specific time which survive the trap can be related to the instantaneous growth rate.

The residence time distribution function $F(t)$ is the fraction of particles which reside in a vessel for a period of time less than t. For a well-stirred vessel this function is

$$F(t) = 1 - e^{-t/\theta'} \tag{59}$$

where θ' is a draw-down time, and for this analysis is based on the volumetric flow to the nuclei trap. If the critical size for removal is denoted as r_c, we can denote the fraction of newly formed nuclei lost to the trap as

$$\text{Fraction lost} = 1 - e^{-\frac{r_c}{G(c)\theta'}} \tag{60}$$

since we have made the quasi steady state assumption over this small time period. Therefore the net nucleation rate for the crystallizer and associated nuclei trap is

$$\text{Net nucleation} = B(c)\, e^{-\frac{r_c}{G(c)\theta'}} \tag{61}$$

To determine the stability of this system we can utilize the previously derived analysis presented in the beginning of this section. All we need do is use Equation (61) as the nucleation function in determining the sensitivity parameter b/g. We see then that for this case

$$\frac{b}{g} = \frac{\bar{G}}{\bar{B}} \frac{\frac{dB}{dc}(\bar{c})}{\frac{dG}{dc}(\bar{c})} + \frac{r_c}{\theta' \bar{G}} \tag{62}$$

whereas for operation without the fines trap

$$\frac{b}{g} = \frac{\overline{\overline{G}}}{\overline{\overline{B}}} \frac{\frac{dB}{dc}(\overline{c})}{\frac{dG}{dc}(\overline{c})} \tag{63}$$

all the terms being evaluated at the steady state.

At a specified solute concentration the value of Equation (62) is always larger than Equation (63). Alternately, from Equation (42) we see that the critical supersaturation level, beneath which cycling occurs, is higher when a nuclei trap is added to the system. Since the steady state solute concentration is slightly increased when a nuclei trap is added to the system, a specification must be set for the two modes of operation before a comparison can be made as to their relative stability.

A meaningful comparison between operation with and without a fines trap is to specify that with the same feed composition, the same product should be produced (for example, the same weight mean particle size). Since the supersaturation is greater with the operation of a fines trap than without, the production rate will also be greater for this case. It is shown in Appendix *A* that for this case, the addition of a fines trap to a crystallizer to produce the same product at a higher capacity will not reduce the stability of the system, and in some cases would improve it. This conclusion has been reached just for the case where the trap is continuously operated and it should be noted that the results could be quite different when the trap is operated on an on-off basis under operator control.

NONLINEAR SOLUTIONS

Clear Feed

In the previous sections, the stability of the system was analyzed by linearization of the equations. This allows one to predict the general effect of the physical parameters on the system and is especially useful when investigating the possibility of stabilizing such a crystallizer by changing the crystallization conditions, seeding, or some feedback control. However in order to understand the complete behavior of the system it is illuminating to solve the complete nonlinear set of equations which can only be done numerically (or on an analog computer).

The starting point of the following analysis is the system of Equations (22), without the seed terms.

$$\frac{d\mu_n}{dt} = nG\mu_{n-1} + (1 - K\mu_3) Br_0^n - \frac{\mu_n}{\theta} \quad n = 0, 1, 2, 3 \ldots \tag{64}$$

$$(1 - K\mu_3) \frac{dc}{dt} = \frac{c_0 - c}{\theta} - (\rho - c)(3K\mu_2 + (1 - K\mu_3) BKr_0^3) \tag{65}$$

To simplify the study of dynamic behavior of this type of system, the variables are normalized about the steady state variables corresponding to the feed concentration c_0 and rate ω. If the feed concentration and rate vary periodically, their mean values can be used as reference points.

Instead of defining the concentration variable as being the ratio of absolute concentration divided by the steady state value, which would be extremely close to 1 at all times, the normalized supersaturation will be followed in time.

The following dimensionless groups are defined:

$$Z_n = \frac{\mu_n}{\overline{\mu}_n} \quad n = 0, 1, 2 \ldots .$$

$$Y = (c - c_s)/(\overline{c} - c_s) \tag{66}$$

where c_s is constant since the system is isothermal.

Since the feed concentration and rate can vary with time, we define

$$j(\tau) = \frac{\omega(\tau)}{\overline{\omega}}$$

$$h(\tau) = \frac{c_0(\tau)}{\overline{c}_0} \tag{67}$$

$$\tau = t\,\overline{\omega}/V = t/\theta$$

where $\overline{c}_0$ and $\overline{\omega}$ are the average values of these inputs. If the feed conditions are constant $j(\tau)$ and $h(\tau)$ are 1.

If these groups are substituted into (64) and (65), along with the dimensionless steady state groups defined in (35) and (36), we get

$$\frac{dZ_n}{d\tau} = L_n \left(\frac{G}{\overline{\overline{G}}}\right) Z_{n-1} + \left(\frac{B}{\overline{\overline{B}}}\right) \frac{R_n}{1 - \varepsilon} - \left(\frac{B}{\overline{\overline{B}}}\right) R_n Z_3 - Z_n j(\tau) \quad n = 0, 1, 2 \ldots .$$

and recognizing that $dc/dt = d(c - c_s)/dt$, we get

$$(1 - (1 - \overline{\varepsilon}) Z_3) \frac{dY}{d\tau} = j(\tau) \left[h(\tau) \frac{\overline{c}_0 - c_s}{\overline{c} - c_s} - Y\right] + j(\tau)\,[h(\tau) - 1] \frac{c_s}{\overline{c} - c_s} - \left[\frac{\rho - c_s}{\overline{c} - c_s} - Y\right] \times \left[L_3 \left(\frac{G}{\overline{\overline{G}}}\right)(1 - \overline{\varepsilon}) Z_2 + (1 - (1 - \overline{\varepsilon}) Z_3) R_3 \left(\frac{B}{\overline{\overline{B}}}\right)\right] \tag{68}$$

The two concentration groups in Equation (68)

$$\frac{\overline{c}_0 - c_s}{\overline{c} - c_s} \quad \text{and} \quad \frac{\rho - c_s}{\overline{c} - c_s}$$

can be rearranged in terms of groups previously defined in the stability study. When we take the kinetic growth model to be linear in supersaturation

$$G = K_1 (c - c_s) \tag{38}$$

then as before

$$g = \frac{1}{\overline{\overline{\varepsilon}}} \frac{\overline{c}_0 - \overline{c}}{\overline{c} - c_s} \tag{39}$$

and

$$\frac{\overline{c}_0 - c_s}{\overline{c} - c_s} = \frac{c_0 - \overline{c}}{\overline{c} - c_s} + 1 = 1 + \overline{\overline{\varepsilon}}\, g \tag{69}$$

and substituting Equation (26) (with $\varepsilon_0 = 1.0$) into the second group, we get

$$\frac{\rho - c_s}{\overline{c} - c_s} = \frac{\rho - \overline{c}}{\overline{c} - c_s} + 1 = \frac{c_0 - \overline{c}}{\overline{c} - c_s} \frac{1}{1 - \overline{\varepsilon}} + 1 = \frac{\overline{\varepsilon}}{1 - \overline{\varepsilon}}\, g + 1 \tag{70}$$

and

$$\frac{G}{\overline{\overline{G}}} = \frac{K_1 (c - c_s)}{K_1 (\overline{c} - c_s)} = Y \tag{71}$$

Also, by assuming a Volmer nucleation model, and remembering we are assuming that c/c_s is close to 1, we can write the nucleation rate as

$$B = K_2\, e^{-\frac{K_3}{[\ln c/c_s]^2}} \approx K_2\, e^{-\frac{K_3}{(c/c_s - 1)^2}} \tag{40}$$

and in conjunction with the linear growth model

$$\frac{b}{g} = \frac{2K_3}{\left(\frac{\bar{c}}{c_s} - 1\right)^2} \tag{42}$$

so we can substitute for the following groups $(c_s/\bar{c} - c_s)$ and $B/\bar{B}$

$$\frac{c_s}{\bar{c} - c_s} = \left[\frac{b/g}{2K_3}\right]^{1/2} \tag{72}$$

$$\frac{B}{\bar{B}} = e^{\frac{1}{2}\frac{b}{g}\left(1-\frac{1}{Y^2}\right)} \tag{73}$$

and substitute (69) to (73) back into (68)

$$\frac{dZ_n}{d\tau} = Y L_n Z_{n-1} + e^{\frac{1}{2}\frac{b}{g}\left(1-\frac{1}{Y^2}\right)} \left[\frac{R_n}{1-\bar{\varepsilon}} - R_n Z_3\right] - Z_n j(\tau) \quad n = 0, 1, 2, 3, \ldots \tag{74}$$

$$(1 - (1-\bar{\varepsilon})Z_3)\frac{dY}{d\tau}[h(\tau)(\bar{\varepsilon}g + 1) - Y] + j(\tau)[h(\tau) - 1]\left[\frac{b}{g} \Big/ 2K_3\right]^{1/2} - \left[\frac{\bar{\varepsilon}}{1-\bar{\varepsilon}} g + 1 - Y\right] \times \left[L_3 Y(1-\bar{\varepsilon})Z_2 + (1-(1-\bar{\varepsilon})Z_3) R_3 e^{\frac{1}{2}\frac{b}{g}\left(1-\frac{1}{Y^2}\right)}\right] \tag{75}$$

This set of equations describes the behavior of the system relative to its steady state in terms of the parameters used in the linear stability analysis (remembering L_n is a function of α and R_n is a function of α and $\bar{\varepsilon}$). Therefore with the linear growth model, the modified Volmer nucleation model, and the assumption of steady state feed conditions ($j(\tau)$ and $h(\tau)$ equal to 1.0), we see the relative dynamic behavior is determined *exactly* by the same variables which determine stability (α, g, $\bar{\varepsilon}$, b/g), while for time varying feed conditions, the constant K_3 must also be known.

Alternately, if the metastable nucleation model were used, the term $(B/\bar{B})$ could be arranged

$$\left(\frac{B}{\bar{B}}\right) = \left(\frac{Y - 1 + \frac{m}{b/g}}{m \Big/ \frac{b}{g}}\right)^m \qquad Y > 1 \tag{76}$$

indicating that in comparison with the Volmer model, the behavior of the system depends on an additional parameter m, which does not appear in the linear stability analysis. The advantage of using the Volmer model which, in most cases, fits the data equally well is that the number of dimensionless groups is reduced. We will later show that in this case the dimensionless behavior of most crystallizers can be characterized by a single dimensionless group b/g which is relatively insensitive to the kinetic model chosen.

Equation (68), along with appropriate nucleation models and an initial perturbation, were solved numerically with the City College IBM 7040 computer.

In all cases in which the system parameters indicated linear stability, initial perturbations were indeed damped out. Furthermore, it was found that in all cases for which the system parameters indicated linear instability, limit cycles developed for any size perturbation. This indicates that the regions mapped out by the linearized stability analysis are representative of the behavior of the actual system.

Limit cycle behavior is caused by operation at a point where the nucleation function is very sensitive (high b/g) which causes the system to give rise to a shower of nuclei when the equilibrium concentration has been exceeded. These nuclei then grow, supplying so much area for growth that the solute concentration decreases below its equilibrium value. This in turn causes the generation of much less than the equilibrium supply of nuclei. Continued withdrawal of crystals from the system reduces the available area for growth and this causes the solute concentration to rise, which again results in a shower of nuclei and repitition of the cycle. Figure 7 demonstrates just this behavior for a typical limit cycle.

The remainder of the work presented in this section focused on the properties of these limit cycles.

The majority of the numerical work done with the nonlinear system Equations (74) and (75) utilized the modified Volmer nucleation model. For this choice of kinetic model [which includes a linear growth model (38)], the nonlinear system is completely defined by the dimensionless groups used in the linearized stability analysis.

Other interesting properties were predicted by Figures 2 and 3 which required corroboration by studying the behavior of the nonlinear system. Specifically, for values of g greater than about 100, the linearized stability indicated that the critical value of b/g was independent of g and that the critical value of b/g was independent of $\bar{\varepsilon}$. Numerous results did indeed indicate for moderately high values of g that the normalized dynamic behavior of the system is independent of g and $\bar{\varepsilon}$.

Since the assumption of $g > 10^2$ is realized for most crystallization systems, the dynamic behavior of the system relative to its predicted steady state becomes a function of only two variables (b/g and α). Then once α has been specified, the value of b/g is the only parameter of importance in determining the limit cycle behavior of the systems.

It was mentioned previously that for a different choice of the nucleation model such as the metastable model, an additional dimensionless group m was introduced. One would, however, expect, from the results based on the modified Volmer model, that the effect of changing m, while keeping b/g constant, should be negligible. This is due to the fact that both nucleating functions are similar near the so-called metastable region and it would be hard to differentiate between them on the basis of experimental data.

The effect of m on the limit cycle was evaluated by determining numerically how the parameters of the limit cycle varied as a function of m. For values of g and α for which the critical value of b/g is independent of g and $\bar{\varepsilon}$, the effect of changing m on the parameters of the limit cycle was negligible.

Curves describing the behavior of the limit cycles are presented in Figures 8, 9, and 10 for α values of 0.0 and 0.1. Actually, the nuclei formed in most systems are so small that they can be taken to be approximately zero.

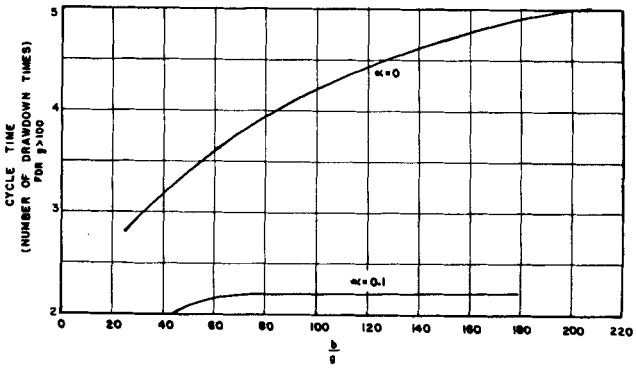

Fig. 8. Cycle time vs. b/g for $g > 100$.

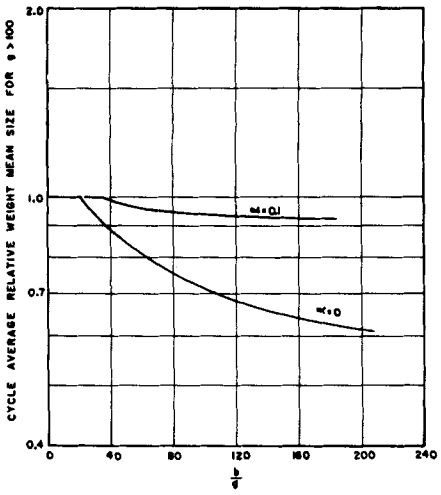

Fig. 9. Cycle average relative weight mean size (Z_4/Z_3) vs. b/g.

Figure 8 shows the relation between cycle time and b/g, and Figure 9 is a graph of the cycle average relative weight mean size vs. b/g (both for $g > 10^2$).

The cycle average relative weight mean size is the average of Z_4/Z_3 over a cycle and is indicative of a composite of continuously sampled material.

As the sensitivity of the system increases (b/g gets greater), a small excess value of Y (relative supersaturation) causes a larger amount of new nuclei (the maximum value of the zero moment increases), requiring a longer interval of time to withdraw the crystals before another shower can take place. This increase of b/g also raises the average surface area present over a cycle, thereby lowering the weight mean product size. Both these effects are shown in Figures 8 and 9.

The effect of increasing the size of α is to damp the amplitude of the zero moment. This is due to the increased size of the nuclei which when formed rapidly reduce the supersaturation, causing less nuclei to be formed during a disturbance than would be for a system with an α of zero. This in turn means that the cycle time will be shorter and the relative weight mean size larger than for a system with a negligible α. This is also shown by Figures 8 and 9. However for α to have an appreciable effect it would have to be much larger than normally encountered during crystallization.

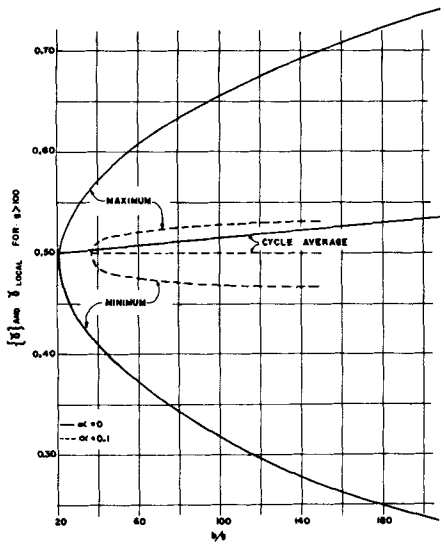

Fig. 10. Cycle average and local coefficient of variation of the weight distribution vs. b/g.

Figure 10 relates the local and cycle average (composite) coefficient of variation of the weight distribution to b/g. This indication of the "tightness" of the distribution is equal to 0.5 for a crystallization system operating in the steady state (both for $\alpha = 0.0$ and 0.1). It is shown in Appendix B that the composite value of γ can never be better than the steady state value. The actual composite value of γ when $\alpha = 0.0$, is only slightly greater than 0.5, while when $\alpha = 0.1$ the difference from 0.5 could not even be noticed. Therefore on a time-averaged basis the nonstable system gives nearly as good a product as does a stable system.

Stabilization by Seeding

There is much practical experience in industry which indicates that adding seed to an oscillating crystallizer will stabilize its operation. The results of the last section seem to corroborate this.

If one had an oscillating system at hand it would be interesting to learn just how much seed of what size would be necessary to stop the oscillations and how the resulting product distribution would change. We have performed this analysis for one case where the initial steady state parameters were $\alpha = 0$, $\bar{\varepsilon} = 0.8$, $g = 500$, $b/g = 50$. These parameters represent an unstable system as can be seen from Figure 2. From Figure 9 it is seen that the resulting product distribution has a cycle average weight mean size of only 85% of that predicted by the steady state equations. Figure 10 shows that substantial local fluctuations in the coefficient of variation will occur while the resulting average is only slightly higher than that of steady state operation.

To perform the calculation we assumed a linear growth model and modifier Volmer nucleation model such that the group b/g is equivalent to that given in Equation (42). The volumetric feed rate remained constant and for each seed size a trial and error calculation was performed to determine how much seed was necessary to stabilize the system. When this was found the weight mean size relative to that predicted by the initial, but unstable, steady state could be calculated. Other properties such as the coefficient of variation and the feed voidage, the latter being an indication of lost productivity as it becomes less than 1, were also calculated.

The results of these calculations are shown in Figure 11. It can be seen for values of β below 1 there is an imperceptibly small difference in the resulting weight mean size, variance, or productivity as compared with the initial, but unattainable, steady state values. The reason for this is that the final steady state has a lower supersaturation than the original unseeded steady state had (final b/g equals 54, original equalled 50), which results in a lower nucleation rate, thus tending to offset the effect of seed addition.

It appears therefore that seed addition is an excellent solution to end cycling performance by both stabilizing the operation and increasing the weight mean size of the product without any significant loss of production.

The results of this study can also be used to analyze the performance of an imperfectly mixed crystallizer. For example, poor mixing at the feed inlet would lead to local high supersaturation levels and local high nucleation rates

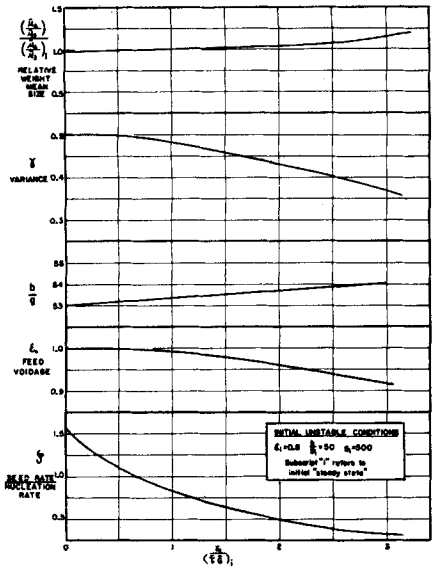

Fig. 11. Effect of seed size stabilization.

while the rest of the crystallizer is well mixed. This kind of system is analogous to a seeded feed into a well-mixed crystallizer, indicating why many commercial installations are free of the problem of cycling.

DISCUSSION OF RESULTS

As mentioned in the introduction, it is well established that continuous crystallizers exhibit cycling behavior. The occurrence of cycling behavior is probably much more frequent than is realized. As shown in the analysis the cycle period is very long, about three to five times the solids' draw-down times. Such long cycles might therefore involve several operator shifts and the cycle itself might be strongly perturbed or masked by changes introduced by the operator. Depending on the control strategy used by the operator, this might enhance instability or just cause an increased variability in the size distribution.

The data available in the literature from which one can calculate values of b/g for a particular system are extremely sparse. However, the two sources which we found both agree with the results of this study.

1. Robinson and Roberts (*13*) fitted a metastable model to an ammonium sulfate system they were operating in their plant. The plant crystallizer was well stirred and did not classify the product. Utilizing Equation (44) and their model, we were able to determine that b/g for this system was greater than 20. Instability and long-term transients were reported for this system, and to calculate the steady state particle distribution an average of sixty-one samples was taken over a period of days.

According to the results of this study, the stability limit for this type of operation is a b/g of about 21 and in all likelihood the instability reported for this system was inherent to the system rather than due to the operators. The fact that they obtained a steady state particle balance which fitted steady state theory only by averaging their results over a period of days is also predicted by this study, as shown in Figure 10.

2. The study of Bransom (*21*) with a well-stirred isothermal salting out crystallizer provides the best data available in the literature. He studied a cyclonite system with the supersaturation provided by the addition of alcohol. By fitting a modified Volmer model to his data, we found that b/g never exceeded a value of 4.0 for the conditions of his study. Consequently, no cycling problem was reported and a particle size distribution was attained which fit steady state theory without averaging. Residence times were very low for this study (about 15 min.) and the product crystal was therefore very small. Calculations indicate that if the residence time were increased to about 1 hr. (which would increase the product size), the stability limits would be reached and any attempt to grow still larger crystals would result in cycling.

SUMMARY AND CONCLUSIONS

The analytical treatment given in this paper provides a basis of understanding the general nature of these phenomena. It is seen that the dominating source of this unstable behavior is the strongly nonlinear nature of the dependence of nucleation rate on supersaturation which, in an oversimplified form, is sometimes described by assuming the existence of a metastable region in which no nucleation occurs. The larger the particle size the lower must be the nucleation rate, and therefore for large crystals one has to operate at supersaturations close to the so-called metastable region. A small upset at these conditions will cause a temporary increase in nucleation rate. Now as the excess amount of nuclei grows the total area increases and the supersaturation decreases, reducing the nucleation rate. However, this effect occurs with a considerable time delay as the new nuclei have no appreciable surface for a considerable time span. Therefore, before the stabilizing action occurs a large number of nuclei might be formed which later will reduce the supersaturation so much that the solution becomes metastable and nucleation practically ceases. At some later time the total surface starts to decrease due to the removal of crystals from the crystallizer in the outflow and the supersaturation starts to increase again.

This leads therefore to the occurrence of limit cycles whose specific properties were described in the analytical part and can be summarized as follows.

Both the tendency to instability and the relative amplitude of the limit cycles increase with increasing b/g and therefore with increasing particle size, at otherwise constant conditions: (1) The free volume or the magma density has little effect on stability limits. (2) The cycle period is comparatively long (three to five times the draw-down time). (3) The instabilities tend to decrease the average particle size and increase the total variance. However, if an individual sample is withdrawn, chances are high that its size distribution will be more uniform than for a Poisson distribution. (4) Correct feeding of the seed will tend to stabilize the system and increase particle size. (5) The total crystal mass will in most cases remain almost constant.

In all the analysis it was assumed that the crystallizer is an ideally stirred tank. It should be pointed out in all fairness that for many crystallizers this is not a good approximation. In this model any incoming feed will become immediately dispersed. In reality this takes a finite mixing time varying from a fraction of a second to several seconds, depending on the size of the vessel (mixing time increases with vessel size (*16*)). With the use of such a model for a regular first- or second-order chemical reaction with a residence time large as compared with the mixing time, the error introduced by neglecting this short initial mixing period is often negligible. In any phenomena involving nucleation the increase in rate of nucleation during this period might be so large that almost all of it will occur during that stage.

Therefore one has to be very careful in using such a model in crystallization. In particular it is doubtful if one can calculate nucleation rates from the overall performance of such crystallizers, as has been suggested.

The deviation of an actually mixed crystallizer from that

of an ideally mixed one will therefore depend both on the nature of the crystallizing solution and on the initial mixing time and therefore on the size of the vessel. The latter factor explains some of the special difficulties encountered in the scale-up of crystallizers.

This deviation from ideal mixing will have a similar effect as that of seeding and will have some stabilizing action. However, even in a case where there are considerable deviations between the actual behavior of the crystallizer and the ideally mixed theoretical model, the present analysis should still present the correct trends and provide an understanding of the phenomena leading to the cyclic behavior of crystallizers.

ACKNOWLEDGMENT

The writers are indebted to their friends at the American Cyanamid Company, and especially to H. M. Hulburt (now at Northwestern University), for their help with the early phases of this work.

The work reported here was supported in part under National Science Foundation Grant No. GK 943.

NOTATION

a = constant in size-dependent growth model, Equation (39)
b = dimensionless nucleation sensitivity group
B = nucleation rate per volume of solution
c = solute concentration in the crystallizer
c_0 = solute concentration in the feed
c_m = metastable concentration
c_s = solubility concentration of the solute
$f(r, t)\,dr$ = number of crystals per unit volume having radii in the range r, $r + dr$ at time τ
$F(t)$ = fraction of particles residing in a vessel for a period of less than t
g = dimensionless growth sensitivity group
G = crystal growth rate dependence on concentration
$h(\tau)$ = normalized feed concentration
$j(\tau)$ = normalized feed rate
K = crystal shape factor
K_n = constants
L_n = steady state dimensionless groups dependent on α
m = exponent in metastable nucleation function
$p(\tau)$ = dimensionless feed rate for stability analysis
$q(\tau)$ = dimensionless feed concentration for stability analysis
r = characteristic radius of the crystal
r_c = nuclei trap cutoff size
r_0 = nuclei characteristic radius
r_s = seed size
r_{wm} = mean particle size with regard to the weight distribution
R_n = steady state dimensionless groups dependent on α and ε
t = time
$\bar{v}$ = partial molar volume of solute
V = crystallizer working volume
$W(r)\,dr$ = crystal weight per volume having radii in the range r, $r + dr$
Y = normalized supersaturation
Y' = dimensionless concentration perturbation
Zn = normalized moments
Zn' = dimensionless moment perturbations

Greek Letters

α = dimension group as defined in Equation (25), $r_0/\tau G$
β = dimension group as defined in Equation (37), $r_s/\tau G$
γ = coefficient of variation
ε = fractional volume of solution
ε_0 = fractional volume of solution in feed
ζ = ratio of seed rate to nucleation rate
η_n = n^{th} moment of ψ
θ = crystallization draw-down time = V/w
θ' = draw-down time based on feed to the nuclei trap
μ_n = n^{th} moment of $f(r)$
ρ = crystal density
τ = dimensionless time
ϕ = crystal growth rate dependence on r
$\psi(r, t)\,dr$ = number of crystals per volume of feed having radii in the range r, $r + dr$, at time t
ω = volumetric feed and/or withdrawal rate

Subscripts

0 = properties of feed
1 = properties of take off

Superscripts

$\bar{\ }$ = steady state values
$'$ = perturbation from steady state
$\{\}$ = cycle average
$\langle\rangle$ = integral over r weighted by f

LITERATURE CITED

1. Aris, Rutherford, and N. R. Amundson, *Chem. Eng. Sci.*, **7**, Pt. I-3, No. 3, 121 (1958).
2. Bransom, S. H., *Brit. Chem. Eng.*, **12**, 838 (1960).
3. ———, et al., *Discussions Faraday Soc.*, **5**, 83 (1949).
4. Cannon, K. J., and N. R. Amundson, *AIChE J.*, **9**, 297 (1963).
5. Crocco, N., and S. Cheng, "Rocket Instability," Butterworths, London (1956).
6. Finn, R. K., and R. E. Wilson, *Agr. Food Chem.*, **2**, No. 2, 66 (1954).
7. Han, C. D., and Reuel Shinnar, paper presented at the 61st National AIChE Meeting, Houston, Texas (February, 1967).
8. Hulburt, H. M., and Stanley Katz, *Chem. Eng. Sci.*, **19**, 555 (1964).
9. McCabe, W. L., and R. P. Stevens, *Chem. Eng. Progr.*, **47**, No. 4, 168 (1951).
10. Miller, P., and W. C. Saeman, *ibid.*, **43**, No. 12, 667 (1947).
11. Murray, D. C., and M. A. Larson, *AIChE J.*, **11**, No. 4, 728 (1965).
12. Randolph, A. D., and M. A. Larson, *ibid.*, **8**, No. 5, 639 (1962).
13. Robinson, J. N., and J. E. Roberts, *Can. J. Chem. Eng.*, **10**, 5 (Oct., 1957).
14. Rumford, F., and J. Bain, *Trans. Inst. Chem. Engrs.*, **38**, 10 (1960).
15. Saeman, W. C., *AIChE J.*, **2**, No. 1, 107 (1956).
16. Shinnar, Reuel, *J. Fluid Mech.*, **10**, Pt. 2, 259–275 (1961).
17. Tanimoto, A., K. Kobayashi, and S. Fujita, *Intern. Chem. Eng.*, **4**, No. 1, 153 (1964).
18. Thomas, W. M., and W. C. Mallison, *Petrol. Refiner*, No. 5, 211 (1961).
19. Van Hook, A., "Crystallization: Theory and Practice," ACS Monograph 152, p. 94, Reinhold, New York (1961).
20. *Ibid.*, p. 13.
21. Worden, R. B., and N. R. Amundson, *Chem. Eng. Sci.*, **17**, 725 (1962).

APPENDIX A.

Operation with and without a fines trap to produce the same product a comparison of stability

In the following let all parameters related to operation with a fines trap be denoted by a subscript f. We can write the nucleation rates for the two modes of operation as follows, using Equations (40) and (61), and assuming c/c_s is close to 1:

$$B_f = K_2\, e^{-\frac{K_3}{\left(\frac{c_f}{c_s}\right)^2}}\, e^{-\frac{r_c}{\theta' G_f}} \qquad (1A)$$

$$B = K_2\, e^{-\frac{K_3}{\left(\frac{c}{c_s}-1\right)^2}} \qquad (2A)$$

Assuming a linear growth model [Equation (38)], we can evaluate the sensitivity parameter b/g for the two modes of operation as described in Equations (62) and (63):

$$\left(\frac{b}{g}\right)_f = \frac{2K_3 c_s^2}{(c_f - c_s)^2} + \frac{r_c}{\theta' G_f} \tag{3A}$$

$$\left(\frac{b}{g}\right)' = \frac{2K_3 c_s^2}{(c - c_s)^2} \tag{4A}$$

In order for the product to be the same for the two modes of operation, we require the weight mean size (μ_4/μ_3) to be the same.

From Equations (25) (unseeded), this yields

$$\theta_f G_f = \theta G \tag{5A}$$

The similarity condition also requires the nucleation rate to be proportional to the feed rate or inversely proportional to the residence time so that

$$\frac{B_f}{B} = \frac{\theta}{\theta_f} \tag{6A}$$

and combining (5A) and (6A)

$$\frac{B_f}{G_f} = \frac{B}{G} \tag{7A}$$

Now ratioing $(b/g)_f$ and (b/g) from Equations (3A) and (4A), we get

$$\frac{(b/g)_f}{(b/g)} = \left(\frac{c - c_s}{c_f - c_s}\right)^2 + \frac{r_c/\theta' G_f}{(b/g)} \tag{8A}$$

From Equation (38) it can be seen that

$$\left(\frac{c - c_s}{c_f - c_s}\right)^2 = \left(\frac{G}{G_f}\right)^2 \tag{9A}$$

So that substitution of Equation (9A) and then (7A) into (8A) yields

$$\frac{(b/g)_f}{(b/g)} = \left(\frac{B}{B_f}\right)^2 + \frac{r_c/\theta' G_f}{(b/g)} \tag{10A}$$

Substitution of (1A) and (2A) into (10A) results in

$$\frac{(b/g)_f}{(b/g)} = e^{-\frac{b}{g}\left[\frac{(b/g)_f}{(b/g)} + \frac{r_c/\theta' G_f}{(b/g)} - 1\right]} + \frac{r_c/\theta' G_f}{(b/g)} \tag{11A}$$

We now wish to know if, with realistic values for $r_c/\theta' G_f$ and (b/g), the ratio $(b/g)_f/(b/g)$ will depart greatly from 1. Values of this ratio greater than 1 indicate a decreasing stability, while values less than 1 indicate the opposite.

Values for $r_c/\theta' G_f$ of 1.0 and 2.38 refer to 67 and 91% fines removal, respectively. With the assumption that the initial system is at the stability borderline (b/g near 20), the term $(r_c/\theta' G_f)/(b/g)$ would have a value in the range of 0.05 to 0.10 for the fines removal rates indicated above. With these values Equation (11A) can be solved, and it is found that the ratio $(b/g)_f/(b/g)$ is slightly smaller than 1, indicating that the addition of a fines trap will not itself cause instability but would actually improve the stability of the system.

APPENDIX B.

Relation of the cycle average coefficient of variation to the steady state value

This relation is derived for the case when $\alpha = 0$ and the feed is clear. For a crystallizer, the supersaturation is so small that μ_3 or ε is taken as a constant.

Steady State

$$\gamma^2 = \frac{\dfrac{\mu_5}{\mu_3} - \left(\dfrac{\mu_4}{\mu_3}\right)^2}{\left(\dfrac{\mu_4}{\mu_3}\right)^2} = \frac{\mu_3 \mu_5}{\mu_4^2} - 1 \tag{1B}$$

Substitution of the relations of (25) for the steady state moments gives

$$\gamma^2 = \frac{5}{4} - 1 = \frac{1}{4}$$

$$\gamma = 0.5$$

Calculation will show that even for values of $\alpha = 0.1$, the steady state coefficient of variation will still be 0.5.

Limit Cycle Average

The average of a moment taken over a limit cycle of time (θ) can be written as

$$\{\mu_n\} = \frac{1}{\theta}\int_t^{t+\theta} \mu_n \, dt$$

In order to get a composite value for the coefficient of variation over the limit cycle, the cycle average variance should be evaluated with respect to the cycle average weight mean size.

$$\{\gamma^2\} = \frac{\dfrac{\{\mu_5\}}{\mu_3} - \dfrac{\{\mu_4\}^2}{\mu_3^2}}{\dfrac{\{\mu_4\}^2}{\mu_3^2}} \tag{2B}$$

When $r_0 = 0$ and the feed is clear, the moment equations for μ_4 and μ_5 can be written from Equation (12) as

$$\frac{d\mu_4}{dt} = 4G\mu_3 - \frac{\omega}{V}\mu_4 \tag{3B}$$

$$\frac{d\mu_5}{dt} = 5G\mu_4 - \frac{\omega}{V}\mu_5 \tag{4B}$$

When a periodic solution is assumed for μ_n, integration of these equations over a cycle gives for Equation (4B)

$$\int_t^{t+\theta} \frac{d\mu_5}{dt}\,dt = \mu_5\Big|_t^{t+\theta} = 0 = 5\theta\{G\mu_4\} - \frac{\omega}{V}\theta\{\mu_5\} \tag{5B}$$

$$\{\mu_5\} = 5\frac{V}{\omega}\{G\mu_4\}$$

Substituting this into (2B), we get

$$\{\gamma^2\} = \frac{5\dfrac{V}{\omega}\mu_3\{G\mu_4\}}{\{\mu_4\}^2} - 1 \tag{6B}$$

Multiplying (3B) by μ_4 and integrating over the cycle, we get

$$\mu_4\frac{d\mu_4}{dt} = \frac{1}{2}\frac{d(\mu_4)^2}{dt} = 4G\mu_3\mu_4 - \frac{\omega}{V}\mu_4^2$$

$$\frac{1}{2}\int_t^{t+\theta}\frac{d\mu_4^2}{dt}\,dt = 0 = 4\mu_3\{G\mu_4\} - \frac{\omega}{V}\{\mu_4^2\} \tag{7B}$$

$$\{G\mu_4\} = \frac{\omega}{V}\{\mu_4^2\}/4\mu_3$$

and substituting (7B) into (6B)

$$\{\gamma^2\} = 5\frac{\{\mu_4^2\}}{\{\mu_4\}^2} - 1 \tag{8B}$$

Subtraction of the steady state γ^2 from $\{\gamma^2\}$ results in

$$\{\gamma^2\} - \gamma^2 = \frac{5}{4}\left[\frac{\{\mu_4^2\}}{\{\mu_4\}^2} - 1\right]$$

The term in parenthesis is the coefficient of variation of μ_4 and since $\{\mu_4^2\} \geq \{\mu_4\}^2$, it is apparent that the accumulated product from a limit cycle will not be tighter than the product from steady state operation. Generally μ_4 does not fluctuate very much and therefore the cycle average $\{\gamma\}$ will be close to the steady state value of 0.5 as shown in Figure 6.

Manuscript received August 18, 1966; revision received January 27, 1967; paper accepted March 28, 1967. Presented at AIChE Philadelphia meeting.